

Structural Optimization of Azadipeptide Nitriles Strongly Increases Association Rates and Allows the Development of Selective Cathepsin Inhibitors

Maxim Frizler, Friederike Lohr, Norbert Furtmann, Julia Kläs, and Michael Gütschow*

Pharmaceutical Institute, Pharmaceutical Chemistry I, University of Bonn, An der Immenburg 4, D-53121 Bonn, Germany

Received October 6, 2010

Using the example of cathepsin K, we demonstrate the design of highly potent and selective azadipeptide nitrile inhibitors. A systematic scan with respect to P2 and P3 substituents was carried out. Structural modifications strongly affected the enzyme–inhibitor association (but not dissociation) rate. A combination of optimized P2 and P3 substituents with a methylation of the P3–P2 amide linker resulted in the picomolar cathepsin K inhibitor **19** with remarkable selectivity over cathepsins L, B, and S.

Introduction

Cysteine cathepsins show a high degree of similarity and play a significant role in many (patho)physiological processes such as bone remodeling, antigen presentation, osteoporosis, autoimmune disorders, and cancer.¹ Therefore, cathepsins represent important targets for new therapeutic strategies.² Inhibitors of cysteine cathepsins are mainly peptidic or peptidomimetic structures containing electrophilic groups prone to covalent interactions with the active-site cysteine. Among them, nitrile-based inhibitors receive the most attention in current drug discovery. Nitriles inhibit cysteine proteases by the reversible formation of a thioimidate adduct resulting from the nucleophilic attack of the active-site cysteine at the nitrile carbon.² The design of peptidomimetic cathepsin inhibitors has usually been based on the structure of their natural substrates. In substrates of proteases, amino acid residues to the N-terminus of the scissile bond are designated P1, P2, etc. The corresponding complementary regions of the enzyme's active site are numbered S1, S2, etc. The S2 pocket represents the best defined subsite of cysteine cathepsins with endopeptidase activity and determines their primary substrate specificity.

Azapeptides have attracted much interest due to their unique properties and applications as peptidomimetics in a variety of biological systems.³ Recently, we have reported on proteolytically stable azadipeptide nitriles as a novel class of cysteine protease inhibitors with picomolar K_i values toward therapeutically relevant cathepsins K, S, and L that form reversible isothiosemicarbazide adducts with the target enzymes. These azadipeptide nitriles were composed of a Cbz-protected P2 amino acid and a P1 aza-amino nitrile, whose nitrogens are essentially alkylated for reasons of the synthetic access.⁴ Despite their excellent inhibitory activity, the reported azadipeptide nitriles were nonselective and it remained unclear whether selectivity for a single target cathepsin can be achieved at all with this class of inhibitors. Using the example of cathepsin K, an approach for the development of selective azadipeptide nitrile inhibitors is reported herein.

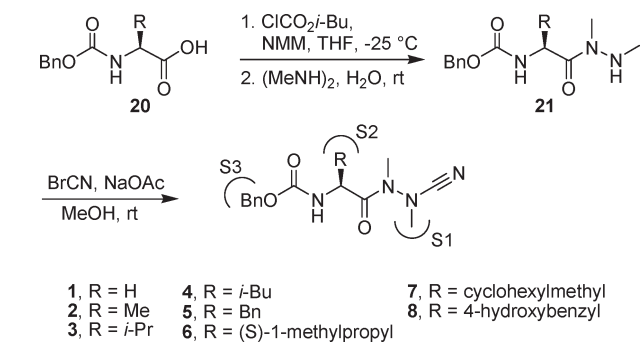
Results and Discussion

We initiated our study with a systematic scan for P2 substituents of the azadipeptide nitrile scaffold. For this purpose, the target compounds **1–3** and **6–8** were prepared as depicted in Table 1 and, together with the known inhibitors **4** and **5**,⁴ tested on human cathepsins L, S, K, and B. Regardless of the substitution pattern, compounds **1–8** displayed a time-dependent slow-binding behavior. Analysis of the progress curves then allows for the determination of the second-order association rate constants (k_{on}) and the first-order dissociation rate constants (k_{off}).⁵ The L-leucine derivative **4** showed strong inhibitory activity and a weak preference for cathepsin K (Table 1). This inhibitor was selected for further optimization of the P3 substituent, while its P2 residue, interacting with the S2 subsite of the proteases, was maintained in all further compounds of this study. The k_{on} values of compounds **1–8** varied considerably depending on the substitution at the P2 position, while the corresponding k_{off} values were in the same range (see Supporting Information, Tables S4, S7). For example, the 17000-fold higher k_{on} value of **4** for cathepsin K, compared to that of the glycine derivative **1** (Table 4), is reflected by the improved potency of **4** (64 pM versus 260 nM, Table 1).

Next, the carbamate group of **4** was replaced by a urea moiety to permit additional hydrogen bond formation. The corresponding azadipeptide nitriles **9** and **10** (Table 2) differ in the length of the P3–P2 linker. The route to the urea-based inhibitors **9** and **10** rests upon the finding that the carbamoyl-protected L-leucine can be converted via mixed anhydride method without racemization.⁶ L-Leucine *tert*-butyl ester **22** (Table 2) was reacted with 1,1'-carbonyldiimidazole (CDI)^a and benzylamine or aniline, respectively. The resulting derivatives **23** were treated with TFA to cleave the *tert*-butyl ester, transformed into the corresponding 1,2-dimethylhydrazides and reacted with cyanogen bromide to obtain **9** and **10** (Table 2). With K_i values of 11 and 17 pM, respectively, compounds **9** and **10** were even more potent for cathepsin K than

*To whom correspondence should be addressed. Phone: +49 228 732317. Fax: +49 228 732567. E-mail: guetschow@uni-bonn.de.

^a Abbreviations: CDI, 1,1'-carbonyldiimidazole; cath, cathepsin; DIPEA, *N*-ethyl-diisopropylamine; DMAP, 4-dimethylaminopyridine; EDC, 1-ethyl-3-(dimethylaminopropyl)carbodiimide; NMM, *N*-methylmorpholine; rt, room temperature.

Table 1. Synthesis of Carbamate-Based Compounds **1–8** and K_i Values

compd	K_i (nM) ^a			
	cath L	cath S	cath K	cath B
1	860	800	260	840
2	480	9.1	33	55
3	1.5	1.5	0.87	4.3
4^b	0.90	0.33	0.064	0.43
5^b	0.16	0.51	0.14	0.68
6	2.6	0.83	0.46	0.88
7	0.40	0.20	0.071	0.48
8	0.36	0.86	0.16	0.38

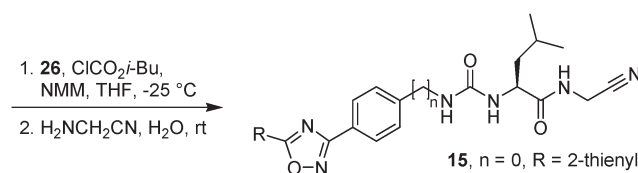
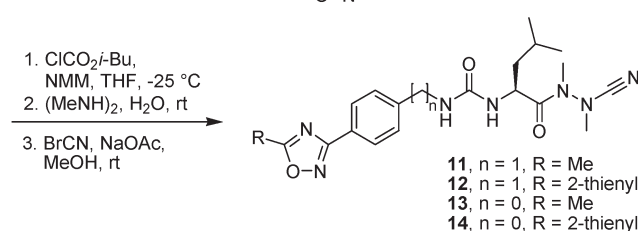
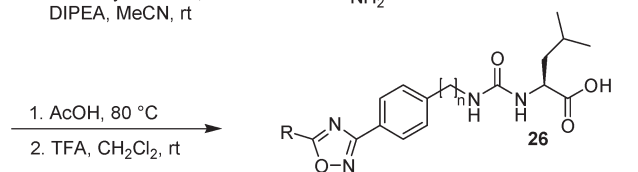
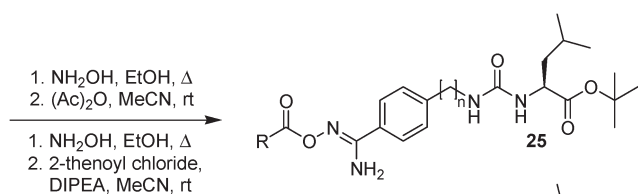
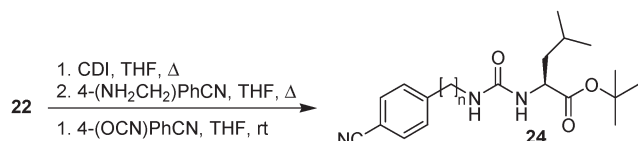
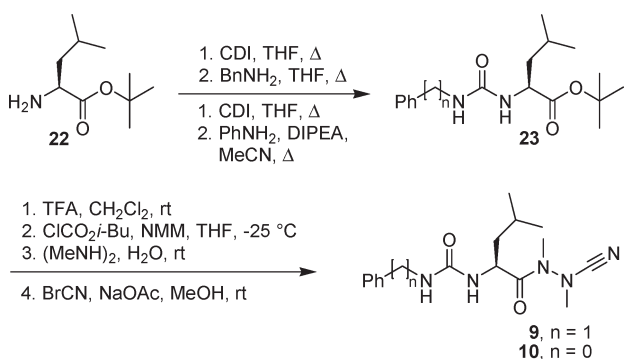
^aThe corresponding standard errors are noted in the Supporting Information (Table S1). ^bLiterature K_i values⁴ for cathepsins L, S, and K have been obtained by a different method.

the corresponding carbamate-based derivative **4** (Tables 1 and 2).

On the basis of recent results on cathepsin K-selective dipeptide nitriles with large biaryl P3 substituents,⁷ we extended the P3 moiety of compounds **9** and **10** to improve the selectivity for cathepsin K over cathepsins L, S, and B. A 1,2,4-oxadiazole heterocycle as a common bioisoster of amide and ester groups⁸ was chosen for the extension. Two benzylurea derivatives bearing a methyl group (**11**) and a 2-thienyl substituent (**12**) in position 5 of the 1,2,4-oxadiazole ring, as well as their phenylurea counterparts **13** and **14**, were synthesized (Table 2). The synthetic route includes the conversion of aromatic nitriles **24** to acyloxyamidines **25**, and the oxadiazole ring closure carried out in acetic acid at 80 °C followed by deprotection with TFA. The final transformations to **11–15** were performed as in the case of **9** and **10**. The exemplary route to **13** is outlined in the Experimental Section.

Inhibitors **11–14** exhibited similar binding affinities with picomolar K_i values on cathepsin K. Triaryl derivatives **12** and **14** were slightly more potent than the methyl substituted biaryl compounds **11** and **13**. Among the six urea-based azadipeptide nitriles, **14** displayed the most promising selectivity profile for cathepsin K over cathepsins L, S, and B (Table 2). The corresponding carba-analogue **15**, prepared from **26** ($n = 0$, R = 2-thienyl) and aminoacetonitrile showed the same trend to selectively inhibit cathepsin K, but with 3 orders of magnitude higher K_i values. A fast-binding inhibition behavior was observed for the carba-analogue **15**, in contrast to the azadipeptide nitriles **9–14**. The k_{on} values of the latter compounds for the four cathepsins reflect the different K_i values (for k_{on} and k_{off} values of **9–14** see Supporting Information, Tables S5, S8).

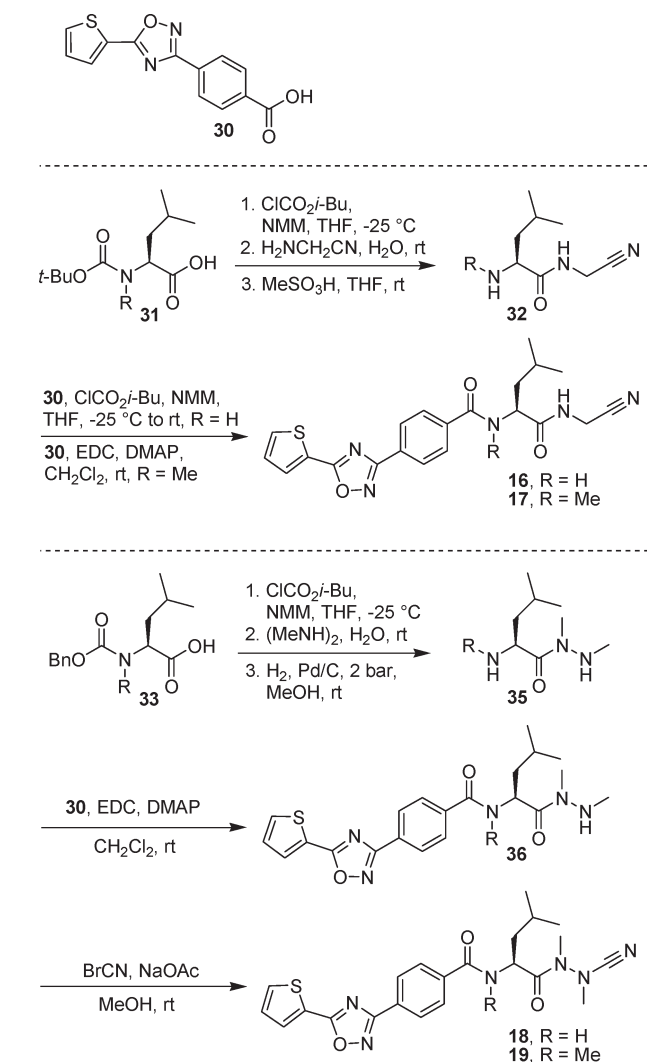
As it became obvious with inhibitor **14**, the combination of the extended P3 triaryl motif with a short P3–P2 linker was advantageous, and we decided to further reduce the linker, leading to the design of amide-based azadipeptide nitriles **18**

Table 2. Synthesis of Urea-Based Compounds **9–15** and K_i Values

compd	K_i (nM) ^a			
	cath L	cath S	cath K	cath B
9	0.39	0.20	0.011	0.65
10	0.045	0.16	0.017	1.3
11	1.4	0.17	0.11	2.8
12	1.1	0.16	0.072	1.3
13	2.0	0.19	0.045	2.4
14	4.4	0.32	0.022	2.4
15	4700	180	34	>22000

^aThe corresponding standard errors are noted in the Supporting Information (Table S2).

and **19** (Table 3). Because of the racemization of *N*-acylamino acids known to occur during the activation of their carboxylic groups, we developed a convergent synthesis for the amide-based compounds. It was first employed for the carba-analogues **16**

Table 3. Synthesis of Amide-Based Compounds **16–19** and K_i Values

compd	K_i (nM) ^a			
	cath L	cath S	cath K	cath B
16	940	140	2.9	>22000
17	>22000	>22000	270	>22000
18	0.22	0.15	0.032	0.36
19	2700	140	0.63	510

^aThe corresponding standard errors are noted in the Supporting Information (Table S3).

and **17** (Table 3). The P3 building block **30** was prepared in five steps with an overall yield of 49% (see Supporting Information). Boc-protected L-leucine (**31**, R = H) and *N*-methyl-L-leucine (**31**, R = Me) were reacted with aminoacetonitrile, followed by removal of the protecting group using methanesulfonic acid and basic extraction to produce **32** (R = H, R = Me). In the final step, building block **30** was activated and coupled with **32** to obtain dipeptide nitriles **16** and **17**.

Similarly, Cbz-protected L-leucine derivatives **33** (R = H, R = Me) were converted into the corresponding 1,2-dimethylhydrazides, whereupon the deprotection was carried out hydrolytically. The coupling products **36** were purified on silica gel and subjected to the final reaction step with cyanogen bromide leading to **18** and **19**. Compounds **16** and **18**, both possessing a CONH linker, showed clear differences in potency, selectivity, and kinetic properties. While the carba-analogue **16**

Table 4. k_{on} Values of Selected Azadipeptide Nitriles

compd	k_{on} ($10^3 \text{ M}^{-1} \text{ s}^{-1}$) ^a			
	cath L	cath S	cath K	cath B
1	0.51	1.7	0.10	0.11
4	620	2000	1700	130
18	800	800	3300	1600
19	nd ^{b,c}	nd ^{b,d}	63	0.62

^aThe corresponding standard errors are noted in the Supporting Information (Tables S4–S6). ^bNot determined. ^cFor [**19**] = 20 μM , a k_{obs} value could not be obtained by nonlinear regression of the progress curves. A limit $k_{\text{obs}}(1 + [\text{S}]/K_m)/[\text{I}] < 1.0 \times 10^3 \text{ M}^{-1} \text{ s}^{-1}$ was therefore estimated. ^dFor [**19**] = 350 nM, a k_{obs} value could not be obtained by nonlinear regression of the progress curves. A limit $k_{\text{obs}}(1 + [\text{S}]/K_m)/[\text{I}] < 20 \times 10^3 \text{ M}^{-1} \text{ s}^{-1}$ was therefore estimated.

with a fast-binding behavior exhibited a 300–7600-fold selectivity for cathepsin K over cathepsins L and B and a moderate selectivity over cathepsin S, the corresponding azadipeptide nitrile **18**, a slow-binding inhibitor, was more potent but much less selective (Table 3). We expected the hydrogen-bond donating CONH linker of **18** to contribute to binding to the four cathepsins studied, whereas the P2 and P3 moieties are already optimized for cathepsin K. Therefore, a methylation to obtain a CONMe linker might be better tolerated by cathepsin K than by the other cathepsins. This was indeed the case. The methylated azadipeptide nitrile **19** still exhibited a picomolar inhibition constant for cathepsin K and a remarkable selectivity over cathepsins L, B, and S (4300-fold, 800-fold, and 200-fold, respectively).

As expected, P3–P2 linker methylation affected the enzyme–inhibitor association rate (**19** versus **18**, Table 4). The *N*-methyl compound **19** showed clearly decreased k_{on} values, reflecting a delayed approach to steady-state. This effect was less pronounced at cathepsin K, for which the optimized substructures, common in **18** and **19**, attenuate the lack of a hydrogen bond formation to the backbone amide of Gly 66⁷ in the case of **19**.

Conclusions

In this study, using the example of cathepsin K, we have demonstrated an approach to design highly potent and selective azadipeptide nitrile inhibitors. Whereas the carba-analogous dipeptide nitriles typically show fast-binding kinetics, a different, slow-binding behavior was observed for azadipeptide nitriles. Thus, it was possible to determine the influence of structural features on association and dissociation rate constants for our series of peptidic nitrile inhibitors. A strong impact of structural variations in azadipeptide nitriles on the enzyme–inhibitor association rate was demonstrated. Although reversibly (see Supporting Information, Figure S3) forming isothiosemicarbazide adducts, these compounds gain their inhibitory activity not only from the covalent attraction but also from specific noncovalent interactions to the active site, as demonstrated herein for azadipeptide nitrile inhibitors for the first time. The dissociation rate, however, was not affected by the compounds' structure. This finding reflects the difficulty in delivering significant binding energy from noncovalent interactions, as discussed for cathepsins and concluded from the large and relatively shallow active site of these target enzymes.^{7,9}

Experimental Section

General. Melting points were determined on a Büchi 510 oil bath apparatus and are uncorrected. Thin layer chromatography was performed on Merck aluminum sheets. Preparative column chromatography was performed on silica gel 60, 0.060–0.200 mm. ¹³C NMR (125 MHz) and ¹H NMR (500 MHz)

spectra were recorded on a Bruker Avance DRX 500 spectrometer. Elemental analyses were performed with a Vario EL apparatus. LC-DAD chromatograms and ESI-MS spectra were recorded on an Agilent 1100 HPLC system with Applied Biosystems API-2000 mass spectrometer. Optical rotation was determined on a Perkin-Elmer 241 polarimeter. IR spectra were recorded on a Bruker Tensor 27 FT-IR spectrometer. Enzymatic assays were performed on a Varian Cary 50 Bio spectrophotometer and a Monaco Safas flx spectrofluorometer. Amino acid derivatives were from Bachem (Bubendorf, Switzerland), Acros (Geel, Belgium), and Aldrich (Steinheim, Germany), and chromogenic and fluorogenic substrates as well as enzymes were obtained from Bachem (Bubendorf, Switzerland), Calbiochem (Darmstadt, Germany), and Enzo Life Sciences (Lörrach, Germany). All tested compounds possessed a purity of not less than 95%.

***N*-(4-Cyanophenylcarbamoyl)-leucine *tert*-Butyl Ester (24, *n* = 0).** The hydrochloride salt of leucine *tert*-butyl ester **22** (5.00 g, 22.3 mmol) was dissolved in dry THF (50 mL) and treated with *N*-ethyl-diisopropylamine (DIPEA) (5.70 mL, 33.3 mmol). The resulting reaction mixture was treated with 4-cyanophenyl isocyanate (3.55 g, 24.6 mmol) and stirred for 4 h at room temperature (rt). After evaporation of the solvent, the residue was suspended in H₂O. The aqueous suspension was adjusted with 10% KHSO₄ to pH ~2 and extracted with ethyl acetate (3 × 30 mL). The combined organic layers were washed with H₂O (20 mL), 10% KHSO₄ (20 mL), H₂O (20 mL), and brine (20 mL). The solvent was dried (Na₂SO₄) and evaporated under reduced pressure. The crude product was recrystallized from ethyl acetate/petroleum ether to obtain **24** (*n* = 0) as a white solid (6.70 g, 91%); mp 113 °C. ¹H NMR (500 MHz, DMSO-*d*₆) δ 0.88 (d, ³*J* = 6.6 Hz, 3H), 0.91 (d, ³*J* = 6.7 Hz, 3H), 1.40 (s, 9H), 1.46–1.54 (m, 2H), 1.62–1.70 (m, 1H), 4.10–4.14 (m, 1H), 6.61 (d, ³*J* = 8.2 Hz, 1H), 7.54 (d, ³*J* = 8.9 Hz, 2H), 7.65 (d, ³*J* = 8.8 Hz, 2H), 9.07 (s, 1H). ¹³C NMR (125 MHz, DMSO-*d*₆) δ 21.82, 22.77, 24.56, 27.78, 40.91, 51.64, 80.85, 102.88, 117.68, 119.48, 133.36, 144.69, 154.40, 172.36.

***N*-(4-Acetoxyamidino)phenylcarbamoyl]-leucine *tert*-Butyl Ester (25, *n* = 0, R = Me).** Compound **24** (*n* = 0; 6.30 g, 19.0 mmol) was dissolved in EtOH (50 mL) and treated with DIPEA (6.46 mL, 37.7 mmol) and hydroxylamine hydrochloride (2.64 g, 38.0 mmol). The resulting solution was heated to reflux overnight. After evaporation of the solvent, the oily residue was dissolved in dry MeCN (50 mL) and treated with acetic anhydride (5.39 mL, 57.4 mmol). The solution was stirred at room temperature for 5 h. The solvent was removed in vacuo, and the oily residue was suspended in H₂O. The aqueous suspension was adjusted with 10% KHSO₄ to pH ~2 and extracted with ethyl acetate (3 × 30 mL). The combined organic layers were washed with 5% KHSO₄ (2 × 30 mL), H₂O (30 mL), satd NaHCO₃ (3 × 30 mL), H₂O (30 mL), and brine (30 mL). The solvent was dried (Na₂SO₄) and removed under reduced pressure. The crude product was recrystallized from ethyl acetate to obtain **25** (*n* = 0, R = Me) as a white solid (5.40 g, 70% from **24**); mp 95 °C. ¹H NMR (500 MHz, DMSO-*d*₆) δ 0.89 (d, ³*J* = 6.6 Hz, 3H), 0.92 (d, ³*J* = 6.6 Hz, 3H), 1.41 (s, 9H), 1.44–1.54 (m, 2H), 1.63–1.71 (m, 1H), 2.11 (s, 3H), 4.11–4.15 (m, 1H), 6.45 (d, ³*J* = 8.2 Hz, 1H), 6.62 (s, 2H), 7.42 (d, ³*J* = 8.9 Hz, 2H), 7.59 (d, ³*J* = 8.9 Hz, 2H), 8.74 (s, 1H). ¹³C NMR (125 MHz, DMSO-*d*₆) δ 20.00, 21.85, 22.77, 24.55, 27.78, 41.07, 51.56, 80.73, 116.98, 124.26, 127.42, 142.28, 154.66, 156.24, 168.65, 172.56.

***N*-[4-(5-Methyl-1,2,4-oxadiazol-3-yl)phenylcarbamoyl]-leucine (26, *n* = 0, R = Me).** Compound **25** (*n* = 0, R = Me; 5.20 g, 12.8 mmol) was dissolved in concentrated acetic acid (40 mL) and stirred at 80 °C for 5 h. After evaporation of the acetic acid, the oily product was dissolved in CH₂Cl₂ (40 mL) and treated with TFA (20 mL). The resulted solution was stirred for 5 h at room temperature. The solvent was evaporated, and the oily residue was suspended in H₂O. The resulting aqueous suspension was extracted with ethyl acetate (3 × 20 mL). The combined organic layers were washed with H₂O (2 × 30 mL) and brine (30 mL). The

solvent was dried (Na₂SO₄) and removed under reduced pressure. The solid product was recrystallized from ethyl acetate/*n*-hexane to obtain **26** (*n* = 0, R = Me) as a white solid (2.80 g, 66% from **25**); mp 156–158 °C. ¹H NMR (500 MHz, DMSO-*d*₆) δ 0.89–0.92 (m, 6H), 1.48–1.58 (m, 2H), 1.65–1.73 (m, 1H), 2.61 (s, 3H), 4.17–4.23 (m, 1H), 6.52 (d, ³*J* = 8.2 Hz, 1H), 7.54 (d, ³*J* = 8.8 Hz, 2H), 7.85 (d, ³*J* = 8.8 Hz, 2H), 8.89 (s, 1H), 12.62 (bs, 1H). ¹³C NMR (125 MHz, DMSO-*d*₆) δ 12.09, 21.76, 22.94, 24.55, 41.05, 50.90, 117.70, 119.00, 127.92, 143.23, 154.70, 167.53, 174.80, 177.05.

***N*-[4-(5-Methyl-1,2,4-oxadiazol-3-yl)phenylcarbamoyl]-leucyl-methylazaalanine-nitrile (13).** Compound **26** (*n* = 0, R = Me; 1.50 g, 4.51 mmol) was dissolved in dry THF (40 mL) and cooled to –25 °C. To the stirred solution, *N*-methylmorpholine (NMM) (0.54 mL, 4.91 mmol) and isobutyl chloroformate (0.65 mL, 4.99 mmol) were added consecutively. 1,2-Dimethylhydrazine dihydrochloride (3.00 g, 22.6 mmol) was suspended in H₂O (3 mL), and 10 N NaOH (5.00 mL) was added under ice-cooling. This solution was given to the reaction mixture when the precipitation of *N*-methylmorpholine hydrochloride occurred. It was allowed to warm to room temperature within 30 min and stirred for additional 90 min. After evaporation of the solvent, the resulting aqueous residue was extracted with ethyl acetate (3 × 30 mL). The combined organic layers were washed with H₂O (30 mL), satd NaHCO₃ (30 mL), H₂O (30 mL), and brine (30 mL). The solvent was dried (Na₂SO₄) and evaporated. The crude product was purified by column chromatography on silica gel using ethyl acetate to obtain *N*-[4-(5-methyl-1,2,4-oxadiazol-3-yl)phenylcarbamoyl]-leucine 1,2-dimethylhydrazide as a colorless oil. Sodium acetate (0.48 g, 5.85 mmol) and cyanogen bromide (0.47 g, 4.44 mmol) were added to a solution of *N*-[4-(5-methyl-1,2,4-oxadiazol-3-yl)phenylcarbamoyl]-leucine 1,2-dimethylhydrazide (1.10 g, 2.94 mmol) in MeOH (30 mL). The mixture was stirred at room temperature for 48 h, and the solvent was removed under reduced pressure. The residue was suspended in H₂O (10 mL), a pH of ~2 was adjusted (10% KHSO₄), and it was extracted with ethyl acetate (3 × 30 mL). The combined organic layers were washed with H₂O (20 mL), satd NaHCO₃ (2 × 30 mL), H₂O (30 mL), and brine (30 mL). The solvent was dried (Na₂SO₄) and removed in vacuo. The oily residue was purified by column chromatography on silica gel using MeOH/CH₂Cl₂ (40:1) as eluent. Additionally, the product was recrystallized from ethyl acetate/petroleum ether to obtain **13** as a white solid (0.66 g, 37% from **26**); mp 185 °C; [α]_D²⁰ = +65.6 (*c* = 0.32, CHCl₃). ¹H NMR (500 MHz, DMSO-*d*₆) mixture of rotamers (only the data of the major rotational isomer are noted) δ 0.93–0.97 (m, 6H), 1.36–1.53 (m, 2H), 1.73 (bs, 1H), 2.62 (s, 3H), 3.11 (s, 3H), 3.27 (s, 3H), 4.80–4.83 (m, 1H), 6.64 (d, ³*J* = 8.2 Hz, 1H), 7.53 (d, ³*J* = 8.5 Hz, 2H), 7.85 (d, ³*J* = 8.8 Hz, 2H), 8.89 (s, 1H). ¹³C NMR (125 MHz, DMSO-*d*₆) δ 12.09, 21.40, 23.29, 24.57, 30.56, 40.46, 40.94, 47.91, 114.22, 117.79, 119.15, 127.92, 142.98, 154.93, 167.50, 174.67, 177.07. FTIR (KBr, cm⁻¹) 2219 (C≡N). LC-ESI/MS (90% H₂O to 100% MeOH in 20 min, then 100% MeOH to 30 min, DAD 239.8–340.8 nm); *t*_r = 21.83, 98% purity, *m/z* = 400.3 ([M + H]⁺).

Acknowledgment. We thank Michael Lülldorff and Patrick Jim Küppers for assistance. This work was supported by the NRW International Research School Biotech-Pharma, Germany.

Supporting Information Available: Inhibition assays and equations, representative plots and detailed kinetic parameters, preparation of compounds **1–36**, as well as ¹H and ¹³C NMR spectra. This material is available free of charge via the Internet at <http://pubs.acs.org>.

Note Added after ASAP Publication. This paper was published ASAP on December 3, 2010 with errors in the footnotes of Table 4, and the Supporting Information file. The correct version was reposted on December 8, 2010.

References

- (1) (a) Lecaille, F.; Kaleta, J.; Brömme, D. Human and parasitic papain-like cysteine proteases: their role in physiology and pathology and recent developments in inhibitor design. *Chem. Rev.* **2002**, *102*, 4459–4488. (b) Brix, K.; Dunkhorst, A.; Mayer, K.; Jordans, S. Cysteine cathepsins: cellular roadmap to different functions. *Biochemie* **2008**, *90*, 194–207. (c) Mohamed, M. M.; Sloane, B. F. Cysteine cathepsins: multifunctional enzymes in cancer. *Nature Rev. Cancer* **2006**, *6*, 764–775.
- (2) Frizler, M.; Stirnberg, M.; Sisay, M. T.; Gütschow, M. Development of nitrile-based peptidic inhibitors of cysteine cathepsins. *Curr. Top. Med. Chem.* **2010**, *10*, 294–322.
- (3) For examples, see (a) Melendez, R. E.; Lubell, W. D. Aza-amino acid scan for rapid identification of secondary structure based on the application of *N*-Boc-aza(1)-dipeptides in peptide synthesis. *J. Am. Chem. Soc.* **2004**, *126*, 6759–6764. (b) Proulx, C.; Lubell, W. D. Aza-1,2,3-triazole-3-alanine synthesis via copper-catalyzed 1,3-dipolar cycloaddition on aza-progargylglycine. *J. Org. Chem.* **2010**, *75*, 5385–5387. (c) Huang, X.; Knoell, C. T.; Hazegh-Azam, M.; Tashjian, A. H.; Hedstrom, L.; Abeles, R. H.; Timasheff, S. N. Modulation of recombinant human prostate-specific antigen: activation by Hofmeister salts and inhibition by azapeptides. Appendix: thermodynamic interpretation of the activation by concentrated salts. *Biochemistry* **2001**, *40*, 11734–11741. (d) Hart, M.; Beeson, C. Utility of azapeptides as major histocompatibility complex class II protein ligands for T-cell activation. *J. Med. Chem.* **2001**, *44*, 3700–3709. (e) Ekici, Ö. D.; Li, Z. Z.; Campbell, A. J.; James, K. E.; Asgian, J. L.; Mikolajczyk, J.; Salvesen, G. S.; Ganesan, R.; Jelakovic, S.; Grütter, M. G.; Powers, J. C. Design, synthesis, and evaluation of aza-peptide Michael acceptors as selective and potent inhibitors of caspases-2, -3, -6, -7, -8, -9, and -10. *J. Med. Chem.* **2006**, *49*, 5728–5749.
- (4) Löser, R.; Frizler, M.; Schilling, K.; Gütschow, M. Azadipeptide nitriles: highly potent and proteolytically stable inhibitors of papain-like cysteine proteases. *Angew. Chem., Int. Ed.* **2008**, *47*, 4331–4334.
- (5) Morrison, J. F.; Walsh, C. T. The behavior and significance of slow-binding enzyme inhibitors. *Adv. Enzymol. Relat. Areas Mol. Biol.* **1988**, *61*, 201–301.
- (6) Lagrille, O.; Taillades, J.; Boiteau, L.; Commeyras, A. *N*-Carbamoyl derivatives and their nitrosation by gaseous NO_x—a new, promising tool in stepwise peptide synthesis. *Eur. J. Org. Chem.* **2002**, 1026–1032.
- (7) Black, W. C. Peptidomimetic inhibitors of cathepsin K. *Curr. Top. Med. Chem.* **2010**, *10*, 745–751.
- (8) Pace, A.; Pierro, P. The new era of 1,2,4-oxadiazoles. *Org. Biomol. Chem.* **2009**, *7*, 4337–4348.
- (9) Cheng, A. C.; Coleman, R. G.; Smyth, K. T.; Cao, Q.; Soulard, P.; Caffrey, D. R.; Salzberg, A. C.; Huang, E. S. Structure-based maximal affinity model predicts small-molecule druggability. *Nature Biotechnol.* **2007**, *25*, 71–75.